



Published in final edited form as:

Bioorg Med Chem. 2004 November 1; 12(21): 5619–5630. doi:10.1016/j.bmc.2004.07.067.

Nucleotide analogues containing 2-oxa-bicyclo[2.2.1]heptane and L- α -threofuranosyl ring systems: interactions with P2Y receptors

Michihiro Ohno^a, Stefano Costanzi^a, Hak Sung Kim^{a,c}, Veerle Kempeneers^d, Karen Vastmans^d, Piet Herdewijn^d, Savitri Maddileti^b, Zhan-Guo Gao^a, T. Kendall Harden^b, and Kenneth A. Jacobson^{a,*}

^aMolecular Recognition Section, Laboratory of Bioorganic Chemistry, NIDDK, National Institutes of Health, Department of Health and Human Services, Bethesda, MD 20892-0810, USA

^bDepartment of Pharmacology, University of North Carolina, School of Medicine, Chapel Hill, NC 27599-7365, USA

^cCollege of Pharmacy and Medicinal Resources Research Center, Wonkwang University, Iksan, 570-749 Chonbuk, South Korea

^dLaboratory of Pharmaceutical Chemistry, Rega Institute for Medical Research, Katholieke Universiteit Leuven, Minderbroedersstraat 10, B-3000 Leuven, Belgium

Abstract

The ribose moiety of adenine nucleotide 3',5'-bisphosphate antagonists of the P2Y₁ receptor has been successfully substituted with a rigid methanocarpa ring system, leading to the conclusion that the North (N) ring conformation is preferred in receptor binding. Similarly, at P2Y₂ and P2Y₄ receptors, nucleotides constrained in the (N) conformation interact equipotently with the corresponding ribosides. We now have synthesized and examined as P2Y receptor ligands nucleotide analogues substituted with two novel ring systems: (1) a (N) locked-carbocyclic (α LNA) derivative containing the oxabicyclo[2.2.1]heptane ring system and (2) L- α -threofuranosyl derivatives. We have also compared potencies and preferred conformations of these nucleotides with the known anhydrohexitol-containing P2Y₁ receptor antagonist MRS2283. A α LNA bisphosphate derivative MRS2584 **21** displayed a K_i value of 22.5nM in binding to the human P2Y₁ receptor, and antagonized the stimulation of PLC by the potent P2Y₁ receptor agonist 2-methylthio-ADP (30nM) with an IC₅₀ of 650nM. The parent α LNA nucleoside bound only weakly to an adenosine receptor (A₃). Thus, this ring system afforded some P2Y receptor selectivity. A L- α -threofuranosyl bisphosphate derivative **9** displayed an IC₅₀ of 15.3 μ M for inhibition of 2-methylthio-ADP-stimulated PLC activity. L- α -Threofuranosyl-UTP **13** was a P2Y receptor agonist with a preference for P2Y₂ (EC₅₀ = 9.9 μ M) versus P2Y₄ receptors. The P2Y₁ receptor binding modes, including rotational angles, were estimated using molecular modeling and receptor docking.

Keywords

Nucleoside; Purine; Pyrimidine; G protein-coupled receptor; Carbocyclic; Phospholipase C; Radioligand binding; Molecular model

1. Introduction

The ribose rings of nucleosides and nucleotides exist in an equilibrium covering a range of conformations, which has been described as a pseudorotational cycle.¹ The North ((N), 2'-*exo*, 3'-*endo*) and South ((S), 2'-*endo*, 3'-*exo*) conformations are the most relevant to the biological activities observed for nucleosides and nucleotides in association with DNA, RNA, and various enzymes.¹⁻⁶

Various ribose ring substitutions have been incorporated into biologically active nucleosides and nucleic acids. A methanocarba modification introduced by Marquez and co-workers^{2,3} has been used to constrain the pseudosugar (cyclopentane) ring of carbocyclic nucleosides in various systems. The methanocarba ring system consists of a fused cyclopropane and cyclopentane rings, to attain either a (N) or (S) conformation depending on the position of fusion. Methanocarba analogues helped to define the role of sugar puckering in stabilizing the active bound conformation at both purine and pyrimidine receptors and thereby allowed identification of a favored conformation.⁴⁻⁶ Using such conformationally constrained analogues, a preference for the (N) conformation of ribose at the P2Y₁ receptor^{5,6} was deduced. The bisphosphate derivatives **1** (MRS2279) and **2** (MRS2500), which are locked in a (N) conformation by the bicyclo[3.1.0]hexane ring system, are the most potent known antagonists of the P2Y₁ receptor (Chart 1).⁶⁻⁹ Subsequently we discovered that P2Y₂, P2Y₄, and P2Y₁₁ receptors can recognize (N)-methanocarba nucleoside 5'-triphosphates **3** and **4** roughly as potently as the corresponding ribosides.⁵ However, in the case of P2Y₆ receptors, the (N)-methanocarba equivalent **5** of the natural nucleotide activator, UDP, was inactive.⁵

In the present study, aimed at further investigating the conformational preferences of P2Y receptors, we have explored additional substitutions of the ribose moiety in P2Y receptor agonists and antagonists.

One such substitution is based on the 'locked nucleic acids' (LNAs), for example, containing monomer **6**, which were introduced several years ago¹⁰⁻¹⁵ and which hybridize effectively to natural RNA. Recently, we reported the synthesis of a novel ring system corresponding to the ring methylene equivalent of the LNAs, that is, carbocyclic LNAs (cLNAs), for example, **7**.¹⁶ cLNAs, which contain the oxabicyclo[2.2.1]heptane ring system, are expected to be more stable than oxygen LNAs because of their nonglycosidic nature, as has been discussed for methanocarba ribose in comparison with natural ribose.^{4,5,17} The cLNA would prefer an approximate (N)-conformation,¹⁶ but is expected to adopt a different pseudorotational angle from that of the (N)-methanocarba ring system.

Another novel ribose substitution adapted to P2Y receptor ligands in the present study is the L- α -threofuranosyl ring. Eschenmoser and colleagues have demonstrated that Watson-Crick pairing in RNA is not exclusively dependent on the ribofuranosyl ring system.^{18,19} The unnatural threofuranosyl ring system (leading to threofuranosyl nucleic acids, TNAs, for example, **8**), which is lacking one carbon in comparison to the ribosyl moiety, is capable of base pairing to RNA strands with a high strength.

Here we report the first synthesis of bisphosphate antagonists of the P2Y₁ receptor **21** and **9**, derived from carbocyclic locked adenine **7** and L- α -threofuranosyl adenine **22**, respectively. These novel ring structures are compared both in biological assays and in P2Y₁ receptor model²⁰ docking with 9-riboside analogues, for example, **10** and **11**, and with a previously reported anhydrohexitol bisphosphate antagonist **12** of the P2Y₁ receptor.⁷ L- α -Threofuranosyl-UTP **13** was also synthesized and assayed at P2Y₂, P2Y₄, and P2Y₆ receptors.

Since the A₃ adenosine receptor (AR)⁴ also showed a preference for the (N) conformation of the ribose, we tested the nucleoside precursors of **2**, **9**, and **21** in binding studies at the ARs.

2. Results

2.1. Chemical synthesis

We prepared *α*LNA analogues of bisphosphate derivatives (Scheme 1), in which the bicyclo[2.2.1]heptane ring system fixed the pseudoribose moiety in a rigid (N)-envelope conformation. Identification of compounds was confirmed by NMR (¹H and ³¹P) and by high-resolution mass spectrometry (HRMS), and purity was demonstrated with high-performance liquid chromatography (HPLC) in two different solvent systems.

In a previous publication,¹⁶ we reported an efficient synthetic procedure for formation of the bicyclo[2.2.1]heptane system. Generally, the formation of carbocyclic nucleosides requires more synthetic steps than does the preparation of the corresponding natural nucleosides. In the reported LNA synthesis^{10,11} the ribose ring was cyclized after introduction of the base. This required more synthetic steps and also made it difficult to synthesize numerous analogues. The coupling of sugar and base moieties at a later stage (Scheme 1) provided greater versatility in the efficient preparation of nucleoside and nucleotide derivatives.

An important aspect in the preparation was the nucleobase synthesis. In this synthesis, we applied a method featuring *N*⁹-protection, as described previously for the synthesis of 2-iodo-6-chloroadenine.⁸ *N*⁹-Protection of the adenine precursor **14** by the pivaloyloxymethyl group, which improved the solubility, enabled various transformation reactions. The 2-iodination of **15a** was then performed by the method of Nair and co-workers.²¹ Treatment of **15b** with methylamine gave 2-iodo-*N*⁶-methyladenine **16** in good yield.

The key step of this synthesis was the coupling of the nucleobase **16** with a triflate intermediate¹⁶ **17** to provide **18**. In a previous study of *α*LNAs,¹⁶ we tried several coupling procedures, but most were unsuccessful because the leaving group was at the concave face of the *α*LNA scaffold, which decreased the reactivity. Only the triflate ester **17** could be applied to this coupling reaction. Also, the coupling step required the use of well-dried potassium carbonate. In the course of this synthesis, the triflate **17** was crystallized from ethyl acetate/petroleum ether. This enabled a large-scale preparation and storage of the triflate substrate as a common intermediate, which is an important advantage in synthetic nucleoside chemistry and in parallel synthesis.

The benzoyl groups of the resulting **18** were hydrolyzed to give **19**. Compound **19** was phosphorylated by the phosphoramidite method to give **20**. The *tert*-butyl protecting group of **20** was removed using trifluoroacetic exchange resin chromatography, to obtain the target compound **21**.

The TNA bisphosphate **9** was prepared as shown in Scheme 2. The synthesis of the UTP analogue **13** was by standard methods of triphosphate formation.³⁴

2.2. Pharmacological activity

We recently developed [³H]MRS2279 **1** as a high-affinity and selective radioligand for quantification of the P2Y₁ receptor.⁹ Therefore, the human P2Y₁ receptor can be expressed from a baculovirus to high levels in Sf9 insect cells, and membranes prepared from these cells can be used with [³H]**1** to directly assess the affinity of newly synthesized molecules at the P2Y₁ receptor. Human P2Y₁ receptor-expressing membranes were incubated with approximately 20nM [³H]**1** and a wide range of concentrations of 2-substituted (N)-methanocarba bisphosphate analogues. The novel *α*LNA adenine nucleotide MRS2584 **21**

interacted with the P2Y₁ receptor, as shown by its capacity to inhibit [³H]**1** binding, and this inhibition occurred with kinetics consistent with interaction at a single site by the law of mass action kinetics. IC₅₀ values were determined from each competition curve, and a K_i value was calculated as 22.5nM according to the relationship $K_i = IC_{50}/1 + [{}^3H]1/K_d$ of [³H]**1**. The K_i value for compounds **9**, **10**, and **12** were also determined, indicating that the riboside **10**, bound more potently than the anhydrohexitol derivative **12** and the TNA bisphosphate **9**, by factors of 5 and 77, respectively.

We also tested the activities of bisphosphate analogues as agonists and antagonists at the human P2Y₁ receptor stably expressed in 1321N1 human astrocytoma cells. Agonist activity was tested by measuring the capacity of the molecules to increase inositol phosphate accumulation by activating the phospholipase C (PLC)-coupled P2Y₁ receptor, and antagonist activity at the P2Y₁ receptor was assessed by measuring the capacity of these molecules to inhibit 2-MeSADP (30nM)-stimulated inositol phosphate accumulation. None of the bisphosphate analogues exhibited agonist activity. The cLNA bisphosphate derivative **21** antagonized the P2Y₁ receptor with an IC₅₀ value of 650nM. The TNA bisphosphate **9** only weakly antagonized the human P2Y₁ receptor with an IC₅₀ value of 15.3μM (Fig. 1). Antagonist potencies at the P2Y₁ receptor for the previously reported⁷ antagonists **10–12** are presented in Table 1 for comparison. Included among the archival compounds was the known anhydrohexitol-containing P2Y₁ receptor antagonist MRS2283 **12**.⁷

Activity of the UTP analogue in the TNA series, compound **13**, was also examined at the PLC-coupled human P2Y₂ and P2Y₄ receptors stably expressed in 1321N1 human astrocytoma cells. The EC₅₀ values for receptor activation by **13** were found to be 9.9 ± 2.1μM (*n* = 3) and 26μM (*n* = 2) at human P2Y₂ and P2Y₄ receptors, respectively (Fig. 2). The corresponding EC₅₀ values for the riboside, UTP, were 8 and 49nM, respectively.⁵ Although **13** was a full agonist at the P2Y₄ receptor, it was completely inactive at the human P2Y₆ receptor.

The adenine nucleosides precursors of **2**, **9**, and **21** were examined in binding to human ARs. Compound **7** (MRS3210), that is, the unsubstituted cLNA adenosine, at 10μM had no effect in binding at two ARs (hA₁, hA_{2A}) and displaced ~30% binding at the hA₃AR. We also tested the corresponding 2-iodo-*N*⁶-methyl nucleoside analogue **19** (MRS3342) in binding assays, and obtained a K_i value of 4.90μM at the hA₃AR. The threofuranosyl adenine nucleoside **22** (which was the precursor of **9**) showed no measurable affinity at 10μM in binding to the hA₁, A_{2A}, A₃ARs or in functional agonism of the hA_{2B}AR. However, the (N)-methanocarba nucleosides typically bind more readily to adenosine receptors and have already been shown to favor selectivity of binding to the A₃AR over other subtypes. (N)-Methanocarba-2-chloro-*N*⁶-methyladenosine, which may be considered the 2'-hydroxy equivalent of the nucleoside precursor of **1**, and thus an (N)-methanocarba analogue of **19** (MRS3342), had a K_i value of 23nM at the hA₃AR and bound more weakly to the rA₁AR.²² Even the parent (N)-methanocarba-adenosine, which was comparable to **7** (MRS3210), had a K_i value of 404nM in binding to the hA₃AR.⁴

2.3. Molecular modeling

With the goal of understanding the molecular features important for the binding of MRS2279 **1**, we studied with computational and molecular biology tools the interactions of **1** with the P2Y₁ receptor.^{20,23} As already stated in the introduction, MRS2279 **1** is a potent and selective P2Y₁ receptor antagonist. We also studied by means of computational techniques the interactions between our rhodopsin-based P2Y₁ model²⁰ and the nonriboside antagonists **2**, **9**, **12**, and **21**. Like **1**, all of these P2Y₁ antagonists may be regarded as

analogues of the 2'-deoxyadenosine-3',5'-bisphosphate in which the 2'-deoxyribose is replaced by various pseudosugar moieties.

The ligands were first fully optimized by means of quenched molecular dynamics and energy minimization. Then they were flexibly superimposed, taking into account both steric and electronic features, to the bound conformation of **1**, as derived from our docking experiments.²⁰ Starting from these ligand/receptor complexes, we carried out automatic docking experiments at the P2Y₁ receptor, to explore the interactions between amino acids in the receptor binding pocket and the various antagonists (Fig. 3). The docking was based on a Monte Carlo/simulated annealing approach. During the docking procedure the ligands and the binding site were treated as fully flexible. In this way we allowed both the receptor and the ligands to undergo the conformational changes necessary for mutual adaptation.

To estimate the conformational changes that the ligands had to go through in order to bind to the receptor, we also studied the sugar puckering of the nucleotides before and after docking at the P2Y₁ receptor by calculating the puckering coordinates of the pseudosugars. The puckering coordinates can be derived from the torsional angles of the rings and furnish a complete description of the puckering. All of the torsional angles could be calculated from the puckering coordinates by applying the inverse formulae. For a description of the puckering of the five-membered rings we used the coordinates P (phase angle of pseudorotation) and θ_m (puckering amplitude) as defined by Altona and Sundaralingham,¹ while for the six-membered ring we used the coordinates Θ (phase angle of symmetrical interconversion), P_2 (phase angle of pseudorotation), and Q (total puckering amplitude) as defined by Haasnoot.²⁴

The special disposition and steric features of the pseudosugar and the phosphate moieties were studied after the superimposition of the adenine moieties of all the docked ligands. This involved analyzing the conformational similarities to the most potent compound **2** (Fig. 4).

As previously observed for **1**, the P2Y₁ receptor binding pocket was identified within the upper regions of the TMs (transmembrane domains) 3, 6, and 7 and the EL2 (the second extracellular loop), with the phosphate moieties coordinated by the essential cationic residues R128(3.29), K280(6.55), and K310(7.39). As in previous models,^{20,23} Q307 (7.36) always acted as a hydrogen bond acceptor from the exocyclic amino group, while S314(7.43) donated a hydrogen bond to N-1 of the adenine moiety. Mutagenesis studies outlined the importance of these five residues for the binding of agonists and antagonists at the P2Y₁ receptor.^{25,26} The N⁶-Me and 2-halo substituents, when present, interacted with Y58(1.39) and Y100(2.53), respectively.

In **2** (Fig. 3a), as in **1**, the 2-deoxyribose was substituted by a methanocarba ring system constrained in the (N) conformation by a (bicyclo[3.1.0]hexane) ring system. The bound conformation of **2** showed a pseudorotational angle (P) of -17° , which indicated an almost pure C2'-*exo* conformation ($P = -18^\circ$). This result was in excellent agreement with the crystal structures of various methanocarba nucleosides developed and analyzed by Marquez and co-workers during the past few years.²⁷ According to the biological data, the (N)-methanocarba ring system confers to the nucleotides the ideal conformation for the interaction with the P2Y₁ receptor.

The bound conformation of **2** showed only minimal deviation from the free ligand optimized in vacuo, indicating that the ligand required small conformational adjustment to fit into binding site of the P2Y₁ receptor and to establish the optimal interactions with the three fundamental cationic residues.

In the case of the *c*LNA analogue **21**, the ribose moiety was replaced by a oxabicyclo[2.2.1]heptane ring system. Like the methanocarba analogues, compound **21** was locked in a (N) conformation by this bicyclic system. However, its bound conformation showed a P of 21° , very close to a pure C3'-*endo* conformation ($P = 18^\circ$). Besides having different P angles, the pseudosugar moieties of the two molecules showed other dissimilarities in overall geometry (Fig. 4). The five-membered ring of **2** tended to be relatively flat, with a θ_m of 31° ; In contrast, in the case of **21** it tended to fold more markedly, showing a θ_m of 60° . Despite these differences, our docking studies suggested that **21** still established interactions with the fundamental cationic residues of TM3, TM6, and TM7 (Fig. 3b). Also in the case of **21**, we detected limited conformational changes between the free ligand optimized in vacuo and the ligand docked into the receptor. The superimposition of the bound conformations of **21** and the potent methanocarba derivative **2** showed a good overlapping of the 5'-phosphate moieties, while greater divergence was found in the position of the 3'-phosphates and in the overall shape of the pseudosugars (Fig. 4a). In particular, the steric hindrance exerted by the bulky 2'-cyclic alkoxy group of **21** on the nearby residues of TM3 could be a possible explanation of the diminished affinity of **21** with respect to its (N)-methanocarba analogue **2**.

The six-membered pseudosugar moiety of the anhydrohexitol derivative **12**, which in the free ligand showed a clear preference for an almost pure chair conformation with a θ of about 0° , after binding to P2Y₁ receptor (Fig. 3c) adopted a O5'-*exo*/C3'-*exo* screw-boat conformation ($\theta = 77^\circ$, $P_2 = -84^\circ$, $Q = 57^\circ$). The superimposition of the bound conformations of **12** and **2** showed a good overlapping of the phosphates and of the pseudosugar moieties, indicating that this anhydrohexitol derivative has the capability to resemble the conformation of the potent (N)-methanocarba analogues (Fig. 4b). The conformational differences that we detected between the P2Y₁ receptor-bound form of **12** and its free form, optimized in vacuo, could be one of the reasons for lower affinity of this compound compared to the (N)-methanocarba analogues.

However, in good agreement with the biological data, the threofuranosyl moiety of **9** did not allow a complete overlapping of the phosphate moieties with those of the most active compounds (**1** and **2**); thus, the interactions with the key cationic residues were not optimal (Fig. 3d). Being unsubstituted at N⁶ and 2 positions, the compound lacked also the favorable hydrophobic interactions with the two Y residues in TM1 and TM2.²⁰ With respect to the conformation of the pseudosugar moiety, we detected a substantial difference between the puckering of the free form of **9** optimized in vacuo ($P = 215$, $\theta_{\max} = 44$), and its P2Y₁ receptor-bound conformation ($P = 260$, $\theta_{\max} = 44$). Nonetheless, the bound compound **9** did not resemble the bound conformation of **2**, but showed significant divergence in the position of the phosphate moieties and in the overall shape of the pseudosugar (Fig. 4c).

3. Discussion

The success of conformationally constrained antagonists in enhancing affinity at the P2Y₁ receptor and the lack of success so far in applying this approach to other P2Y subtypes,⁵⁻⁸ prompted us to search for other (N)-like ring systems, especially those that may adopt a slightly different conformation according to the pseudorotational cycle and therefore may have an altered pharmacological profile.

These potential advantages encouraged us to synthesize ring-constrained carbocyclic-type analogues for improved ligands for the G protein-coupled P2Y receptors by using both novel *c*LNA units of the (N) conformation and L- α -threofuranosyl substitution of ribose as a test of the conformational requirements at the putative binding sites.

According to the biological data and our docking experiments, the (N)-methanocarba pseudosugar moiety seemed to be endowed with a puckering that could ensure an optimal fit of the ligand in the P2Y₁ binding pocket, together with the ideal orientation of the bisphosphates for the interactions with the cationic residues of the binding site. Also, the *c*LNA analogue **21** was locked within a preferred conformation range of the pseudoribose for binding to the P2Y₁ receptor.

The *c*LNA analogue **21** (MRS2584) was an antagonist at the hP2Y₁ receptor and displayed a high binding affinity indicated by a K_i value of 22.5nM. Compound **21** was roughly equipotent with the 2-iodo ribose analogue **11**, which had an IC₅₀ value of 891nM in a functional assay at the turkey P2Y₁ receptor. The nucleotide **21** was 3-fold less potent in binding than the corresponding 2-chloro ribose analogue **10**, which had a K_i value of 8.6nM. In comparison to the methanocarba analogue **2**, the potency of **21** was somewhat diminished. Compound **21** was 29-fold less potent than **2** (MRS2500), which had a K_i value of 0.78nM in binding to the hP2Y₁ receptor. Compound **21** was 9-fold less potent than **1** (MRS2279), which had a K_i value of 2.5nM in binding to the hP2Y₁ receptor.

Previous data indicated that the presence of a ribose 2'-OMe group decreased antagonist potency at the P2Y₁ receptor.³⁵ A 2'-ether group is present in **21**, and the effect of this 2'-cyclic alkoxy group on antagonist potency is unknown. It was also suggested from molecular modeling and docking in the human P2Y₁ receptor (Fig. 3b) that amino acids from TM3, that is, F131(3.32), H132(3.33), and L135(3.36) may have steric interactions with the 2'-substituents. Furthermore, the substitution of the ribose with the oxabicyclo[2.2.1]heptane ring did not allow the optimal orientation of the 3'-phosphate group for interaction with the essential cationic residues.

The adenosine receptor binding results for **19** showed that a *c*LNA scaffold does not fit in the binding site of the hA₃AR as effectively as does the (N)-methanocarba ring system. Thus, the *c*LNA, containing the oxabicyclo[2.2.1]heptane ring system, apparently is a P2 receptor-selective scaffold. The molecular modeling results of the hA₃AR binding site model also indicated a direct interaction of the 2'-OH and 3'-OH groups with Q167(EL2) and H272(7.43). Furthermore, the models suggest that 2'-substitutions may exhibit steric interference with L90(3.32) and L91(3.33) of hA₃AR.^{28,29} On the other hand the (N)-methanocarba moiety exhibited an optimal puckering for interaction with the A₃AR (and to a greater degree than other AR subtypes). Compound **22** (precursor of **9**) was also inactive at adenosine receptors. However, since TNAs only weakly activated the P2Y receptors, a statement about the receptor selectivity of this ring system would not be justified.

The two threofuranosyl derivatives examined in this study only weakly antagonized (**9** at P2Y₁) or activated (**13** at P2Y₂, and P2Y₄ receptors) the P2Y receptors. In good agreement with the biological data, our molecular modeling studies emphasized that the threofuranosyl moiety does not confer to the ligands the steric features necessary for recognition by the P2Y₁ receptor.

In conclusion, we have synthesized a novel (N)-locked carbocyclic bisphosphate using a *c*LNA scaffold. The pseudorotational *P* value of the *c*LNA compound was calculated to be +21° and its conformation belonged to the (N)-(³E) category. This *c*LNA bisphosphate derivative displayed potent binding affinity at the human P2Y₁ receptor. In contrast, the *c*LNA nucleoside bound only weakly to the hA₃AR receptor and did not bind appreciably to other adenosine receptors. Thus, this ring system contributes to selectivity for the P2Y₁ receptor. Thus, the order or suitability of various nonribose ring systems to bind to P2Y₁ receptors was: bicyclo[3.1.0]hexane > 2-oxa-bicyclo[2.2.1]heptane > L- α -threofuranose.

The L- α -threofuranosyl analogue of UTP maintains a preference for activating the P2Y₂ in comparison to the P2Y₄ receptor.

4. Experimental

4.1. Chemical synthesis

Nucleosides and synthetic reagents were purchased from Sigma Chemical Co. (St. Louis, MO) and Aldrich (Milwaukee, WI). Compound **12** was synthesized as described⁷.

¹H NMR spectra were obtained with a Varian Gemini-300 spectrometer (300MHz) with D₂O, CDCl₃, CD₃OD, and DMSO-*d*₆ as a solvent. ³¹P NMR spectra were recorded at room temperature with a Varian XL-300 spectrometer (121.42MHz); orthophosphoric acid (85%) was used as an external standard.

Purity of compounds was checked with a Hewlett-Packard 1090 HPLC apparatus equipped with an SMT OD-5-60 RP-C18 analytical column (250 × 4.6mm; Separation Methods Technologies, Inc., Newark, DE) in two solvent systems. System A: linear gradient solvent system: 0.1M TEAA/CH₃CN from 95/5 to 40/60 in 20min; the flow rate was 1mL/min. System B: linear gradient solvent system: 5mM TBAP/CH₃CN from 80/20 to 40/60 in 20min; the flow rate was 1mL/min. System C: linear gradient solvent system: H₂O/CH₃CN from 95/5 to 0/100 in 30 min; the flow rate was 1mL/min. Peaks were detected by UV absorption with a diode array detector. All derivatives tested for biological activity showed 97% purity in the HPLC systems. Low-resolution CI-NH₃ (chemical ionization) mass spectra were measured with a Finnigan 4600 mass spectrometer and high-resolution EI (electron impact) mass spectrometry was performed with a VG7070F mass spectrometer at 6kV. High-resolution FAB (fast atom bombardment) mass spectrometry was performed with a JEOL SX102 spectrometer with 6kV Xe atoms following desorption from a glycerol matrix. Purification of the nucleotide analogues for biological testing was carried out on Sephadex-DEAE-A-25 resin columns with a linear gradient (0.01–0.5M) of 0.5M ammonium bicarbonate.

4.1.1. (2'R,3'R,4'S)-Phosphoric acid mono-[2-(6-aminopurin-9-yl)-4-phosphonoxy-tetrahydro-furan-3-yl] ester (9)—Compound **23** (10mg, 0.013mmol) was dissolved in a mixture of methanol (2mL) and water (1mL) and hydrogenated over a 10% Pd/C (10mg) at room temperature for 2d. The catalyst was removed by filtration and the methanol was evaporated. The residue was treated with ammonium bicarbonate solution and subsequently frozen and lyophilized. Purification of the obtained residue was performed on an ion-exchange column packed with Sephadex-DEAE A-25 resin, a linear gradient (0.01–0.5M) of 0.5M ammonium bicarbonate was applied as the mobile phase, and UV and HPLC were used to monitor the elution, which furnished **9** (1.8mg, 30%). ¹H NMR (D₂O) δ 8.41 (s, 1H), 8.31 (s, 1H), 6.33 (s, 1H), 5.10 (d, 1H, *J* = 8.7 Hz), 4.93–4.90 (br, 1H), 4.51 (d, 1H, *J* = 10.3 Hz), 4.41 (dd, 1H, *J* = 3.3, 10.3 Hz); ³¹P NMR (D₂O) δ -0.29 (br s); MS (m/e) (negative-FAB) 396 (M⁺-H). HRMS (negative-FAB) calcd for C₉H₁₂N₅O₉P₂ 396.0110. Found 396.0119; HPLC 16.0min (99%) (system B), 2.7min (99%) (system C).

4.1.2. 2-Amino-6-chloropurin-9-yl-methyl 2,2-dimethylpropionate (15a)—2-Amino-6-chloropurine **14** (1.00g, 5.90mmol) was dissolved in DMSO (5.0mL) under heating. DMF (20.0mL), chloromethyl pivalate (1.0mL, 6.94mmol) and K₂CO₃ (990mg, 7.16mmol) were added and the mixture was stirred at room temperature for 3d. The reaction mixture was filtered and the filtrate was evaporated. The obtained residue was purified by flash chromatography (AcOEt/petroleum ether = 2/1) and recrystallized from AcOEt–petroleum ether, which furnished the desired compound **15a** (1.33 g, 79 %). ¹H NMR

(CDCl₃) δ 8.01 (s, 1H), 6.00 (s, 2H), 5.20 (br s, 2H), 1.18 (s, 9H); MS (m/e) (positive-FAB) 284, 286 (peak height ratio is 3:1) (M⁺+H).

4.1.3. 6-Chloro-2-iodopurin-9-yl-methyl 2,2-dimethylpropionate (15b)—To a solution of 2-amino-6-chloropurin-9-yl-methyl 2,2-dimethylpropionate **15a** (704mg, 2.48mmol) in MeCN (2.0mL) was added diiodomethane (8.0mL) and *t*-butylnitrite (0.90mL, 9.99mmol) and oxygen was purged by N₂ bubbling. The tube was sealed and stirred at 80°C for 2.5 h. The solvent was removed under vacuum and the obtained residue was purified by flash chromatography (AcOEt/petroleum ether = 1/2), which furnished **15b** (561mg, 57 %). ¹H NMR (CDCl₃) δ 8.29 (s, 1H), 6.14 (s, 2H), 1.19 (s, 9H); MS (m/e) (positive-FAB) 395, 397 (peak height ratio is 3:1) (M⁺+H).

4.1.4. 2-Iodo-6-methylamino-9H-purine (16)—2,2-Dimethyl-propionic acid 6-chloro-2-iodopurin-9-ylmethyl ester **15b** (148mg, 0.375mmol) was dissolved in THF (2.0mL) and *i*-PrOH (5.0mL) in sealed tube. 40% MeNH₂ in water (1.0mL) was added, and the solution stirred at 60°C for 18h. The precipitate, which formed was filtered and washed with small amount of water to furnish 2-iodo-6-methylaminopurine **16** (102mg, 99%). ¹H NMR (CDCl₃) δ 7.99 (s, 1H), 7.86 (br s, 1H), 2.88 (br s, 3H); MS (m/e) (positive-FAB) 276 (M⁺+H).

4.1.5. (1'S,4'R,6'S,7'S)-Benzoic acid 4-benzoxymethyl-6-trifluoromethanesulfonyloxy-2-oxa-bicyclo[2.2.1]hept-7-yl ester (17)—To a stirred solution of (1'S,4'R,6'S,7'S)-benzoic acid 4-benzoxymethyl-6-hydroxy-2-oxa-bicyclo[2.2.1]hept-7-yl ester¹⁶ (54mg, 0.147mmol) and 4-dimethylaminopyridine (195mg, 1.60mmol) in methylene chloride (6.0mL) was added trifluoromethanesulfonic anhydride (75 μ L, 0.446mmol) at 0°C. After stirring for 10min at 0°C, the reaction mixture was treated with sat NaHCO₃ (2mL) and extracted with chloroform. The organic layer was separated and washed with brine, dried over anhydrous sodium sulfate, filtered, and concentrated. The residue was purified by column chromatography (silica gel, AcOEt/petroleum ether = 5/1–3/1) to give triflate **17** (73.6mg, 99%). ¹H NMR (CDCl₃) δ 8.05–8.01 (m, 2H), 7.99–7.94 (m, 2H), 7.63–7.54 (m, 2H), 7.47–7.39 (m, 4H), 5.33 (ddd, 1H, *J* = 2.2, 2.7, 9.9 Hz), 5.13 (s, 1H), 4.63 (d, 1H, *J* = 2.2 Hz), 4.50 (AB quartet, 2H, *J* = 12.1 Hz), 4.32 (dd, 1H, *J* = 3.3, 7.4 Hz), 4.05 (d, 1H, *J* = 7.4 Hz), 2.56 (ddd, 1H, *J* = 3.3, 10.1, 14.6 Hz), 2.01 (dd, 1H, *J* = 3.0, 14.6 Hz). MS (m/e) (positive-FAB) 501 (M⁺+H).

4.1.6. (1'S,4'R,6'S,7'S)-Benzoic acid 4-benzoyloxymethyl-6-(2-iodo-6-methylaminopurin-9-yl)-2-oxa-bicyclo[2.2.1]hept-7-yl ester (18)—(1'S,4'R,6'S,7'S)-Benzoic acid 4-benzoyloxymethyl-6-trifluoromethanesulfonyloxy-2-oxa-bicyclo[2.2.1]hept-7-yl ester **17** (20mg, 0.040mmol), 2-iodo-6-methylaminopurine **16** (25mg, 0.091mmol), potassium carbonate (18mg, 0.130mmol) and 18-crown-6 (4mg, 0.015mmol) in DMF (0.30mL) was stirred at 60°C for 3h. The resulting mixture was dried up under vacuum, and the residue was purified by silica gel column chromatography (AcOEt) and preparative TLC (silica gel, AcOEt/petroleum ether = 1/1), to give dibenzoyl adenine derivative **18** (23mg, 91%). ¹H NMR (CDCl₃) δ 8.06–7.96 (m, 4H), 7.90 (s, 1H), 7.58 (m, 2H), 7.42 (m, 4H), 5.88 (br s, 1H), 5.64 (s, 1H), 4.80 (dd, 1H, *J* = 5.1, 9.6 Hz), 4.71 (s, 1H), 4.68 (d, 1H, *J* = 11.7Hz), 4.61 (d, 1H, *J* = 11.7 Hz), 4.28 (dd, 1H, *J* = 3.0, 7.2 Hz), 3.97 (d, 1H, *J* = 7.2 Hz), 3.17 (br s, 3H), 2.70 (dd, 1H, *J* = 9.6, 13.8 Hz), 2.33 (m, 1H); MS (m/e) (positive-FAB) 626 (M⁺+H).

4.1.7. (1'S,4'R,6'S,7'S)-6-(2-Iodo-6-methylaminopurin-9-yl)-4-hydroxymethyl-2-oxa-bicyclo[2.2.1]hept-7-ol (19)—A mixture of dibenzoyl adenine derivative **18** (21mg, 0.034mmol), potassium carbonate (17mg, 0.123mmol) in THF (0.5mL) and methanol

(1.0mL) was stirred at room temperature for 25h. The solvent was removed by nitrogen purging and the residue was purified by silica gel column chromatography (MeOH/CHCl₃ = 1/5), to give the cLNA adenine derivative **19** (12.5mg, 89 %). ¹H NMR (CD₃OD) δ 8.03 (s, 1H), 4.63 (dd, 1H, *J* = 6.0, 9.3 Hz), 4.32 (s, 1H), 4.15 (s, 1H), 3.90 (dd, 1H, *J* = 2.1, 6.6 Hz), 3.85 (d, 1H, *J* = 11.1 Hz), 3.73 (d, 1H, *J* = 11.1 Hz), 3.68 (d, 1H, *J* = 6.6 Hz), 3.04 (br s, 3H), 2.41–2.26 (m, 2H); MS (m/e) (positive-FAB) 418 (M⁺+H), HR-MS (positive-FAB) calcd for C₁₃H₁₇N₅O₃I 418.0376. Found 418.0363.

4.1.8. (1'S,4'R,6'S,7'S)-6-(2-Iodo-6-methylaminopurin-9-yl)-4-[(di-*t*-butyl-phosphato)-methyl]-7-(di-*t*-butyl-phosphato)-2-oxa-bicyclo[2.2.1]heptane (20)

—The cLNA adenine derivative **19** (8.2mg, 0.020mmol) and 1*H*-tetrazole (20mg, 0.285mmol) were dissolved in 1.0mL of anhydrous THF. Di-*t*-butyl diethylphosphoramidite (0.055mL, 0.198mmol) was added, and the mixture was stirred for 3h at room temperature. The reaction mixture was cooled to –78 °C and treated with a solution of *m*-CPBA (70% max, 55mg) in CH₂Cl₂ (2.5mL). The resulting mixture was warmed to room temperature and 5% NaHSO₃ (2.0mL) was added. The reaction mixture was stirred another 30min at room temperature and extracted with AcOEt. The organic phase was subsequently washed with saturated aqueous NaHCO₃ and brine, and then dried over Na₂SO₄ and filtered. The solvent was removed under reduced pressure. The residue obtained was purified by silica gel column chromatography (MeOH/CHCl₃ = 1/5), which furnished **20** (10mg, 64%). ¹H NMR (CDCl₃) δ 8.06 (s, 1H), 6.20 (br s, 1H), 4.84 (d, 1H, *J* = 4.8 Hz), 4.67 (m, 2H), 4.21 (m, 2H), 4.00 (m, 1H), 3.82 (d, 1H, *J* = 6.9 Hz), 3.16 (br s, 3H), 2.60–3.50 (m, 1H), 2.40–2.30 (m, 1H), 1.48 (s × 2, 18H), 1.47 (s × 2, 18H); MS (m/e) (positive-FAB) 802 (M⁺+H), 824 (M⁺+Na).

4.1.9. (1'S,4'R,6'S,7'S)-Phosphoric acid mono-[6-(2-iodo-6-methylaminopurin-9-yl)-4-phosphonooxymethyl-2-oxabicyclo[2.2.1]hept-7-yl] ester (21)

—A solution of **20** (8.0mg, 0.011mmol) in 5% TFA/CH₂Cl₂ (1.0mL) was stirred for 2h at 25°C. The solvent was removed under reduced pressure and the residue was quenched by addition of 5.0mL of triethylammonium bicarbonate buffer (1.0M). The mixture was subsequently frozen and lyophilized. Purification of the obtained residue was performed on an ion-exchange column packed with Sephadex-DEAE A-25 resin, a linear gradient (0.01–0.5M) of 0.5M ammonium bicarbonate was applied as the mobile phase, and UV and HPLC were used to monitor the elution, which furnished **21** (5.3mg, 73%). ¹H NMR (D₂O) δ 8.23 (s, 1H), 4.64 (m, 1H), 4.47 (br s, 2H), 4.12 (m, 1H), 3.96 (m, 2H), 3.83 (d, 1H, *J* = 6.9 Hz), 3.09 (br s, 3H), 2.53–2.32 (m, 2H); ³¹P NMR (D₂O) δ 2.22, 1.81 (2s); MS (m/e) (negative-FAB) 576 (M⁺-H); HRMS (negative-FAB) calcd for C₁₃H₁₇N₅O₉P₂I 575.9546. Found 575.9557; HPLC 9.1min (99%) (system A), 15.8min (99%) (system B).

4.1.10. (2'R,3'R,4'S)-Phosphoric acid 2-(6-aminopurin-9-yl)-4-(bis-benzyloxy-phosphoryloxy)-tetrahydro-furan-3-yl ester dibenzyl ester (23)

—To a stirred solution of (2'*R*,3'*R*,4'*S*)-2-(6-aminopurin-9-yl)-tetrahydro-furan-3,4-diol **22** (5mg, 0.021mmol) and 1*H*-tetrazole (13mg, 0.186mmol) in anhydrous THF (2.0mL) was added dibenzyl diisopropylphosphoramidite (22mg, 0.069mmol). After stirring for 3h at room temperature, the reaction mixture was cooled to –78 °C and was treated with a solution of *m*-CPBA (70% max, 25mg) in CH₂Cl₂ (1mL). The resulting mixture was warmed to room temperature, treated with 5% NaHSO₃ (2.0mL) for another 30min at room temperature and extracted with AcOEt. The organic phase was washed with satd NaHCO₃ aq and brine and dried over Na₂SO₄ and filtered. The solvent was removed under reduced pressure. The residue obtained was purified by column chromatography (silica gel, eluent: CHCl₃/MeOH = 10/1), to give **23** (10mg, 63%). ¹H NMR (CDCl₃) δ 8.18 (s, 1H), 7.87 (s, 1H), 7.36–7.19 (m, 20H), 6.51 (br s, 2H), 6.18 (d, 1H, *J* = 1.5 Hz), 5.33 (d, 1H, *J* = 7.5 Hz), 5.07 (m, 4H),

5.00 (br, 1H), 4.91 (m, 4H), 4.31 (d, 1H, $J = 10.8$ Hz), 4.10(dd, 1H, $J = 3.9, 10.8$ Hz); MS (m/e) (negative-CI) 756 ($M^+ - H$).

4.2. Pharmacology

2-MeSADP and GTP were purchased from Sigma (St. Louis, MO). *Myo*-[3H]inositol (20Ci/mmol) was obtained from American Radiolabeled Chemicals (St. Louis, MO).

P2Y receptor-promoted stimulation of inositol phosphate formation was measured at human P2Y₁, P2Y₂, P2Y₄, or P2Y₆ receptors stably expressed in 1321N1 human astrocytoma cells as previously described.^{5,30,31} The IC₅₀ values were averaged from 3 to 8 independently determined concentration–effect curves for each compound. Briefly, cells plated in 24-well dishes were labeled in inositol-free medium (DMEM; Gibco, Gaithersburg MD) containing 1.0 μ Ci of 2-[3H]myo-inositol (20 Ci/mmol; American Radiolabeled Chemicals, Inc., St. Louis MO) for 18–24h in a humidified atmosphere of 95% air/5% CO₂ at 37°C. PLC activity was measured the following day by quantitating [3H]inositol phosphate accumulation after a 10min incubation at 37 °C in the presence of 10mM LiCl. Total [3H]inositol phosphates were quantified by anion exchange chromatography as previously described.^{30,31} The affinities of bisphosphate analogues for the human P2Y₁ receptor were directly determined by using [3H]1 in a radioligand binding assay, as we recently described in detail.⁹ Binding and functional parameters were estimated using GRAPHPAD PRISM software (GraphPAD, San Diego, CA, USA).

4.3. Molecular modeling

Molecular mechanics calculations have been carried out by means of the Discover3 module of INSIGHTII,³² using the CFF91 forcefield.³³ The P2Y₁ model used for the docking experiments was the rhodopsin based homology model previously constructed by us.²⁰ Before performing the docking experiments, the ligands have been optimized by means of a quenched molecular dynamics simulation followed by energy minimization.

An NVT (constant-volume/constant-temperature) molecular dynamic simulation was carried out at constant temperature of 300K for 10ps, using a time step of 1 fs. During the simulation, snapshots of the system were taken at regular intervals of 1ps. The structures in each snapshot were energy minimized (BFGS Newton method) until an RMS (root mean squared) of 0.00001kcal/mol/Å was reached and the one showing the lowest energy was used as starting point for the docking experiments.

The flexible superimpositions have been carried out by means of the FIELDFIT program of Search Compare module of INSIGHTII,³² giving equal weight to the steric and the electrostatic factors. The bound conformation of MRS2279 was kept rigid during the calculation, while the structures to be superimposed were fully flexible. An alignment of the molecules based on their dipole and quadrupole moments was used as the starting position.

The automatic docking experiments were carried out by means of the Monte Carlo minimization/simulated annealing approach implemented in the Affinity module of INSIGHTII. The binding site was defined as all the residues within 6Å distance from the ligands. Full flexibility was granted to the ligands and to the residues of the binding site. All the atoms of the ligands and the key residues of the binding pocket (R128, K280, R310, Q307, S314) capable of donating or accepting hydrogen bonds were manually marked. During the Monte Carlo simulation the scaling factor for the van der Waals term was set at 0.1, while the coulombic and hydrogen bond terms were set at 1. The maximum movement in each random translation and rotation of the ligand were set at 0.1Å and 1°, respectively. Fifty stages of simulated annealing were performed after the Monte Carlo simulation, setting

the initial temperature at 500K, the final temperature at 300K, the final van der Waals and coulombic scaling factors at 1.0 and the final hydrogen bonds scaling factor at 0.0. In other words the van der Waals and coulombic factors were fully considered during the simulated annealing and the hydrogen bond external biases were gradually removed. After the docking procedure, the ligand/receptor complexes were energy minimized until reaching an RMS of 0.05 kcal/mol/Å.

The puckering coordinates P , θ_m , P_2 , Q , and Θ were calculated by means of the formulae:

$$P = \text{atan}\{[(v_4 + v_1) - (v_3 + v_0)] / [2v_2(\sin\pi/5 + \sin2\pi/5)]\}$$

$$\theta_m = v_2 / \cos P$$

$$P_2 = \text{atan}\left[-\left(\sum_{j=0}^5 v_j \sin 2\pi j/3\right) / \left(\sum_{j=0}^5 v_j \cos 2\pi j/3\right)\right]$$

$$Q = \left\{ \left[\left(\sum_{j=0}^5 v_j \cos 2\pi j/3 \right) / (3 \cos P_2) \right]^2 + \left[\left(\sum_{j=0}^5 v_j \cos \pi j \right) / 6 \right]^2 \right\}^{1/2}$$

$$\Theta = \text{atan}\left\{ 2 \left(\sum_{j=0}^5 v_j \cos 2\pi j/3 \right) / \left[\cos P_2 \left(\sum_{j=0}^5 v_j \cos \pi j \right) \right] \right\}$$

which we derived from the works of Altona and Sundaralingham¹ and of Haasnoot.²⁴ The pseudosugar endocyclic torsion angles v_j are numbered according to the IUPAC-IUB recommendations for the conformation of polysaccharide chains (www.chem.qmul.ac.uk/iupac/misc/psac.html). All the angles are expressed in radians.

Acknowledgments

MO is on sabbatical from Toray Industries (Kamakura, Japan) and thanks them for financial support. Mass spectral measurements were carried out by Dr. Victor Livengood and NMR by Wesley White (NIDDK). We thank Prof. A. Eschenmoser and Dr. R. Krishnamurthy of the Scripps Res. Inst. (San Diego, CA) for helpful discussions and for the gift of L- α -threofuranosyl-adenine.

References and notes

1. Altona C, Sundaralingham M. *J Am Chem Soc.* 1972; 94:8205. [PubMed: 5079964]
2. Marquez VE, Siddiqui MA, Ezzitouni A, Russ P, Wang J, Wagner RW, Matteucci MD. *J Med Chem.* 1996; 39:3739. [PubMed: 8809162]
3. Shin KJ, Moon HR, George C, Marquez VE. *J Org Chem.* 2000; 65:2172. [PubMed: 10774042]
4. Jacobson KA, Ji X-D, Li AH, Melman N, Siddiqui MA, Shin KJ, Marquez VE, Ravi RG. *J Med Chem.* 2000; 43:2196. [PubMed: 10841798]
5. Kim HS, Ravi RG, Marquez VE, Maddileti S, Wihlborg A-K, Erlinge D, Malmsjö M, Harden TK, Boyer JL, Jacobson KA. *J Med Chem.* 2002; 45:208. [PubMed: 11754592]
6. Boyer JL, Adams M, Ravi RG, Jacobson KA, Harden TK. *Br J Pharmacol.* 2002; 135:2004. [PubMed: 11959804]

7. Nandan E, Jang SY, Moro S, Kim H, Siddiqui MA, Russ P, Marquez VE, Busson R, Herdewijn P, Harden TK, Boyer JL, Jacobson KA. *J Med Chem.* 2000; 43:829. [PubMed: 10715151]
8. Kim HS, Ohno M, Xu B, Kim HO, Choi Y, Ji XD, Maddileti S, Marquez VE, Harden TK, Jacobson KA. *J Med Chem.* 2003; 46:4974. [PubMed: 14584948]
9. Waldo GL, Corbitt J, Boyer JL, Ravi G, Kim HS, Ji X-D, Lacy J, Jacobson KA, Harden TK. *Mol Pharmacol.* 2002; 62:1249. [PubMed: 12391289]
10. Obika S, Nanbu D, Fari Y, Morio K-I, In Y, Ishida T, Imanishi T. *Tetrahedron Lett.* 1997; 38:8735.
11. (a) Petersen M, Bondensgaard K, Wengel J, Jacobsen JP. *J Am Chem Soc.* 2002; 124:5974. [PubMed: 12022830] (b) Petersen M, Wengel J. *Trends Biotechnol.* 2003; 21:74. [PubMed: 12573856]
12. Koshkin AA, Fensholdt J, Pfundheller HM, Lomholt C. *J Org Chem.* 2001; 66:8504. [PubMed: 11735531]
13. Hodgson DM, Gibbs AR, Drew MGB. *J Chem Soc, Perkin Trans 1.* 1999; 24:3579.
14. (a) Alex G, Kruger AW, Meyers AI. *Tetrahedron Lett.* 2001; 42:4305. (b) Arrington MP, Meyers AI. *Chem Commun.* 1999; 15:1371.
15. Obike S, Morio K-I, Nanbu D, Hari Y, Itoh H, Imanishi T. *Tetrahedron.* 2002; 58:3039.
16. Kim HS, Jacobson KA. *Org Lett.* 2003; 5:1665. [PubMed: 12735747]
17. Ravi RG, Kim HS, Servos J, Zimmermann H, Lee K, Maddileti S, Boyer JL, Harden TK, Jacobson KA. *J Med Chem.* 2002; 45:2090. [PubMed: 11985476]
18. Schöning K, Scholz P, Guntha S, Wu X, Krishnamurthy R, Eschenmoser A. *Science.* 2000; 290:1347. [PubMed: 11082060]
19. Schöning K, Scholz P, Wu X, Guntha S, Delgado G, Krishnamurthy R, Eschenmoser A. *Helv Chim Acta.* 2002; 85:4111.
20. Costanzi S, Mamedova L, Gao ZG, Jacobson KA. *J Med Chem.* (in press).
21. (a) Nair V, Fasbender AJ. *Tetrahedron.* 1993; 49:2169–2184. (b) Nair V, Richardson SG. *J Org Chem.* 1980; 45:3969. (c) Nair V, Richardson SG. *Synthesis.* 1982:670.
22. Lee K, Ravi RG, Ji X-d, Marquez VE, Jacobson KA. *Bioorg Med Chem Lett.* 2001; 11:1333. [PubMed: 11392549]
23. Kim HS, Barak D, Harden TK, Boyer JL, Jacobson KA. *J Med Chem.* 2001; 44:3092. [PubMed: 11543678]
24. Haasnoot CAG. *J Am Chem Soc.* 1993; 115:1460.
25. Moro S, Guo D, Camaioni E, Boyer JL, Harden TK, Jacobson KA. *J Med Chem.* 1998; 41:1456. [PubMed: 9554879]
26. Jiang Q, Guo D, Lee BX, van Rhee AM, Kim Y-C, Nicholas RA, Schachter J, Harden TK, Jacobson KA. *Mol Pharmacol.* 1997; 52:499. [PubMed: 9281613]
27. Choi Y, George C, Comin MJ, Barchi JJ Jr, Kim HS, Jacobson KA, Balzarini J, Mitsuya H, Boyer PL, Hughes SH, Marquez VE. *J Med Chem.* 2003; 46:3292. [PubMed: 12852759]
28. Costanzi S, Lambertucci C, Vittori S, Volpini R, Cristalli G. *J Mol Graph Model.* 2003; 21:253. [PubMed: 12479925]
29. Gao ZG, Kim SK, Biadatti T, Chen W, Lee K, Barak D, Kim SG, Johnson CR, Jacobson KA. *J Med Chem.* 2002; 45:4471. [PubMed: 12238926]
30. Harden TK, Hawkins PT, Stephens L, Boyer JL, Downes P. *Biochem J.* 1988; 252:583. [PubMed: 2843174]
31. Boyer JL, Downes CP, Harden TK. *J Biol Chem.* 1989; 264:884. [PubMed: 2910869]
32. InsightII version 2000.1, Accelrys (former MSI). San Diego, CA:
33. Maple JR, Hwang MJ, Stockfisch TP, Dinur U, Waldman M, Ewig CS, Hagler AT. *J Comput Chem.* 1994; 15:162.
34. Kempeneers V, Froeyen M, Vastmans K, Herdewijn P. *Chem Biodiver.* 2004; 1:112.
35. Nandan E, Camaioni E, Jang SY, Kim YC, Cristalli G, Herdewijn P, Secrist JA, Tiwari KN, Mohanram A, Harden TK, Boyer JL, Jacobson KA. *J Med Chem.* 1999; 42:1625. [PubMed: 10229631]

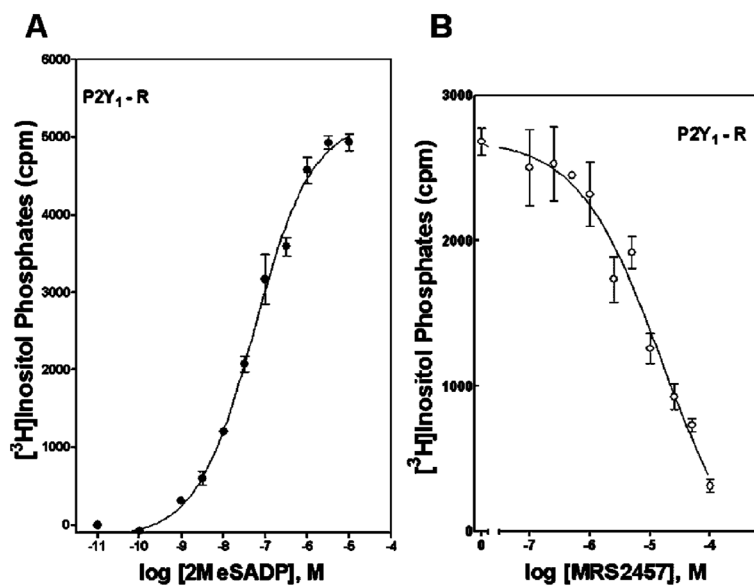


Figure 1.

Activation of the human P2Y₁ receptor (A) and competitive antagonism (B) of 2-MeSADP-promoted activation. PLC activity was measured as described in Section 4 in 1321N1 human astrocytoma cells stably expressing the human P2Y₁ receptor. Assays were in the presence of the indicated concentrations of the agonist 2-MeSADP alone or in the presence of 100nM–100μM MRS2457 **9**. The data are the means of triplicate determinations and are representative of results obtained in three separate experiments.

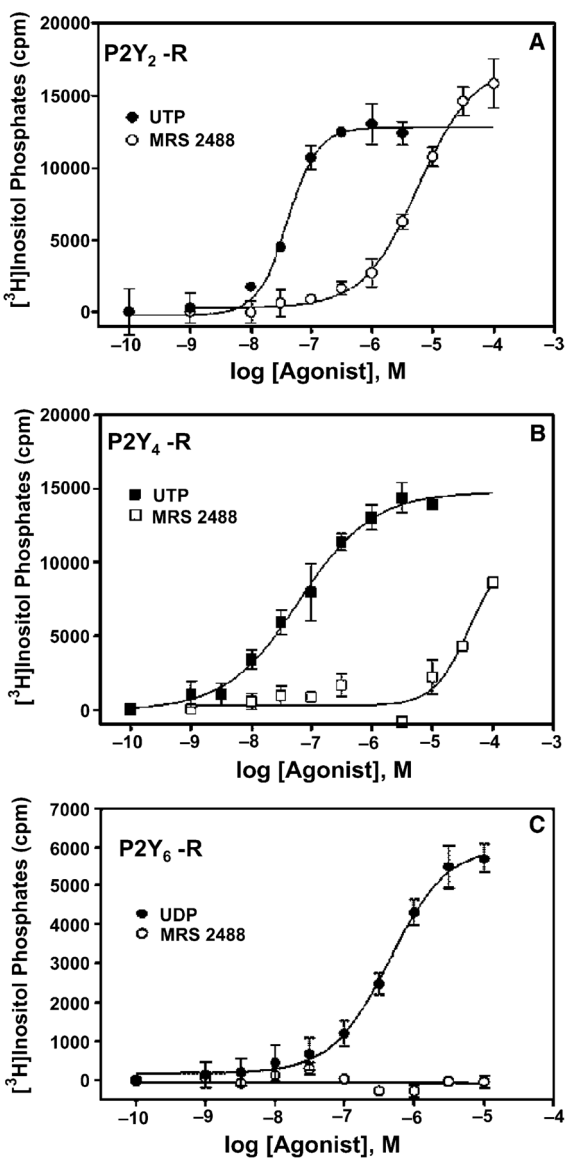


Figure 2. Activation of the human P2Y₂ (A), P2Y₄ (B), and P2Y₆ (C) receptors by the uracil nucleotides UDP and UTP and by the L- α -threofuranosyl analogue of UTP (MRS2488 **13**). PLC activity was measured as described in Section 4 in 1321N1 human astrocytoma cells stably expressing the human P2Y receptors. The data are the means of triplicate determinations and are representative of results obtained in three separate experiments.

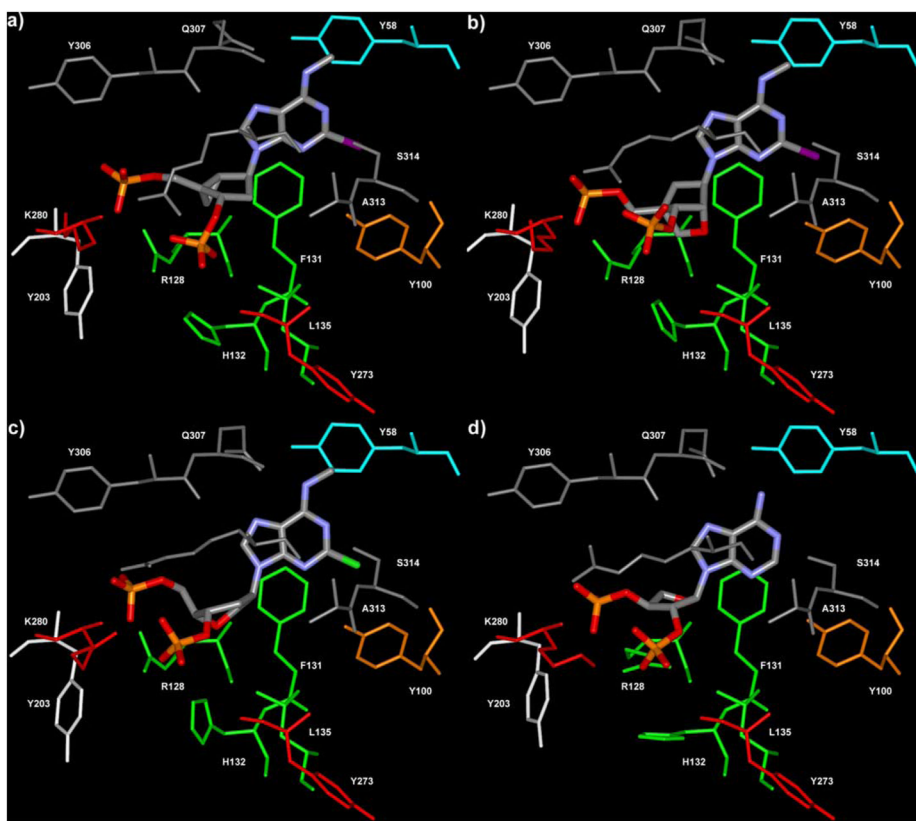


Figure 3. P2Y₁ receptor complexes with the ligands MRS2500 **2** (a), MRS2584 **21** (b), MRS2283 **12** (c), and MRS2457 **9** (d). The residues of the P2Y₁ binding pocket are colored according to the following scheme: cyan (TM1), orange (TM2), green (TM3), red (TM6), gray (TM7), white (EL2).

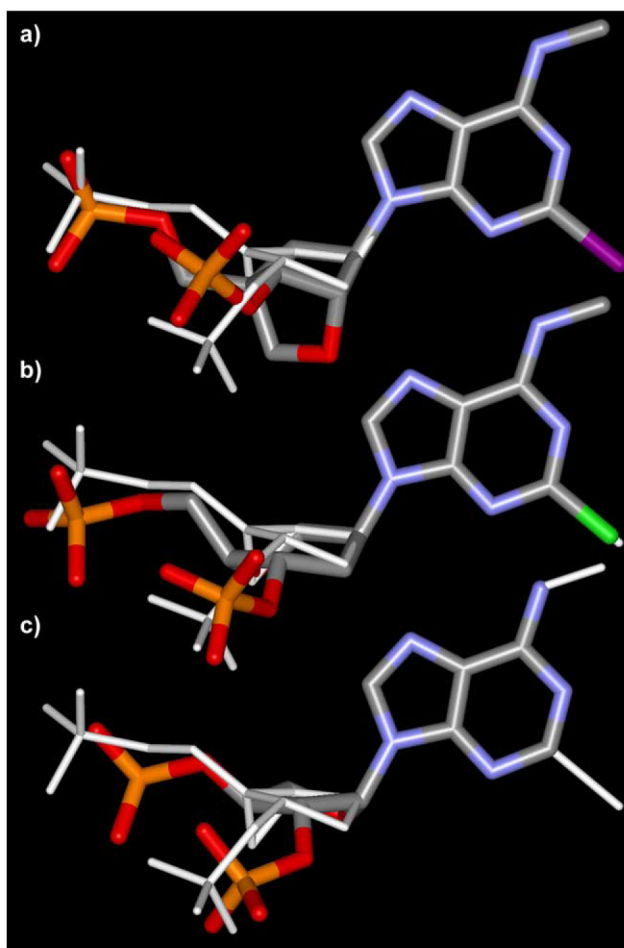
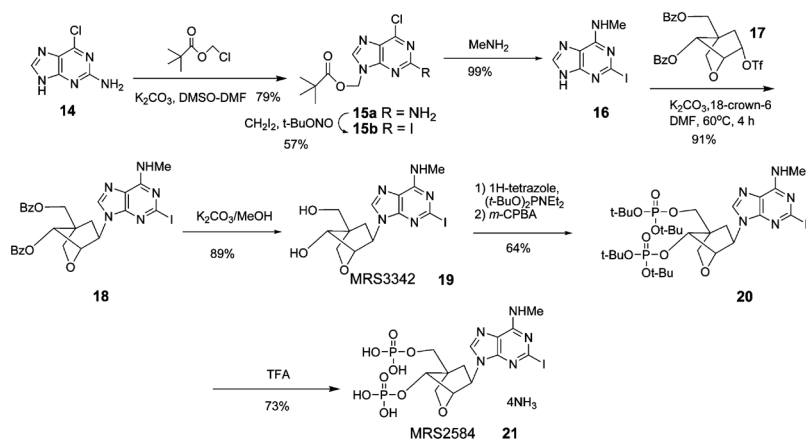
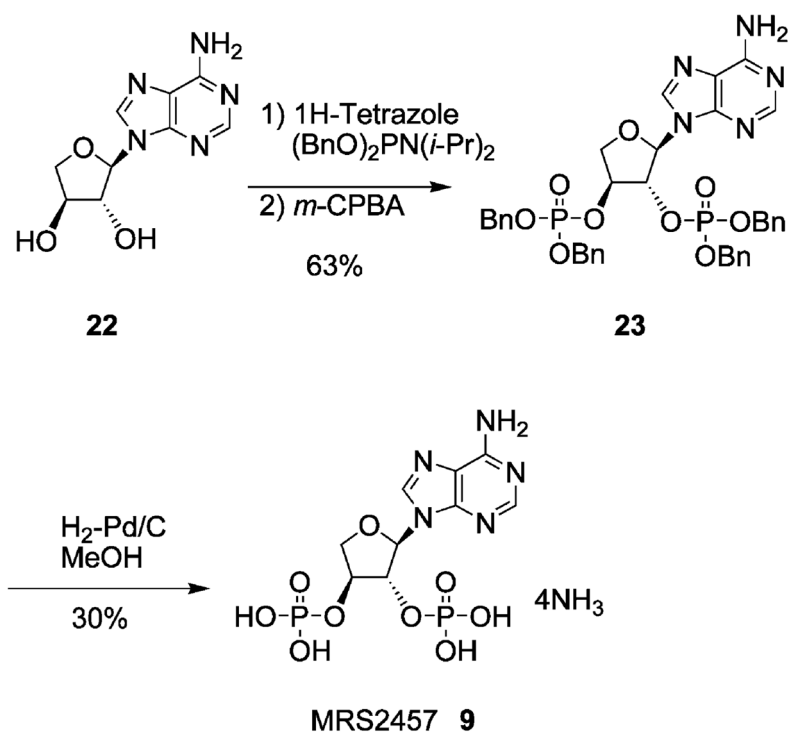


Figure 4. Superimpositions of the bound conformation of MRS2584 **21** (a), MRS2283 **12** (b), and MRS2457 **9** (c) with MRS2500 **2**, performed by overlapping the adenine moieties. The anhydrohexitol derivative **12** can resemble the bound conformation of the most active compound **2**.



Scheme 1.



Scheme 2.

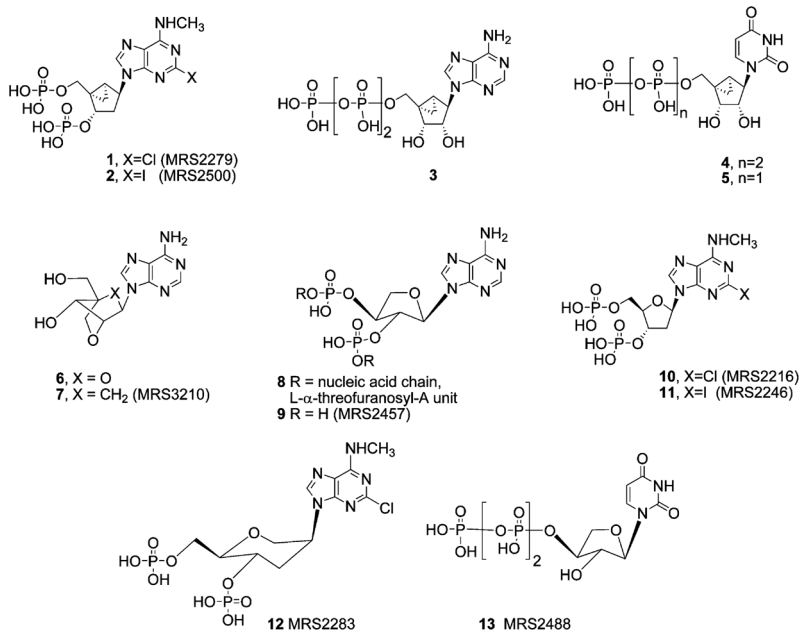


Chart 1.

Table 1

In vitro pharmacological data at P2Y₁ receptors in binding (human receptor expressed in Sf9 cells)⁹ and for inhibition of PLC activity stimulated by 30nM 2-MeSADP (human receptor expressed in 1321N1 astrocytoma cells or in turkey erythrocytes)

Compound	R = (2-position)	R' = (N ⁶ -position)	Binding, K _i , nM ^a	Antagonism, IC ₅₀ , nM ^b
1 MRS2279 ^c	Cl	CH ₃	2.5 ± 0.4	51.6 ± 0.8 (t)
2 MRS2500 ^c	I	CH ₃	0.78 ± 0.08	8.4 ± 0.8 (h)
9 MRS 2457	H	H	666 ± 333	15,300 ± 300 (h)
10 MRS 2216	Cl	CH ₃	8.6 ± 2.6	206 ± 53 (t)
11 MRS 2246	I	CH ₃	ND	891 ± 233 (t)
12 MRS 2283	Cl	CH ₃	43 ± 10	566 ± 224 (t) ^c
21 MRS 2584	I	CH ₃	22.5 ± 10.4	650 ± 100 (h)

Mean ± s.e.m. is given for three separate determinations. None of the compounds displayed agonist effects.

^aThe affinities were determined by using [³H]**1** in a radioligand binding assay, as recently described.⁹ The human P2Y₁ receptor was expressed to high levels in Sf9 insect cells with a recombinant baculovirus. Membranes prepared from these cells were incubated for 30min at 4°C in the presence of ~20nM [³H]**1**.

^bAntagonist IC₅₀ values represent the concentration needed to inhibit by 50% the effect elicited by 30nM 2-MeSADP. *n* = 3, unless otherwise indicated in parentheses. t = turkey, h = human.

^cValues from Refs. [7–9,35]. ND not determined.